JOURNAL OF THERMOPHYSICS AND HEAT TRANSFER
Vol. 10, No. 4, October–December 1996

Efficient Linear Multistep Method for Nonlinear Volterra Integral Equations

Rafael Villasenor*
National Center for Research and Technological Development, 62490 Cuernavaca, Morelos, México
and
Pavel Krutitskii†
Moscow State University, Moscow 119899 Russia

The nonsingular, nonlinear Volterra integral equation of the second kind for the surface temperature of a cylinder with a continuous heat sink is solved numerically by a simple, but robust, procedure based on a composite formula. The present scheme is capable of handling stiff and nonstiff kernels expressed in terms of infinite series that contain standard functions. The numerical method is tested by imposing linear and nonlinear boundary conditions at the cylinder surface. The boundary conditions and source terms are treated explicitly without resorting to a linearization technique. To show the versatility of the numerical scheme, two classes of nonlinear boundary conditions are considered, the Stefan–Boltzmann boundary condition and the time-dependent Newton's cooling law. The accuracy and robustness of the present method for solving Volterra equations of the second kind are verified considering two different forms of the source term. Two additional methods of solution are used in this investigation as benchmarks. One of them is a pseudospectral approach and the other is a standard finite difference calculation. The integral equation scheme is found to work well over the entire nondimensional time domain. Numerical results are presented for a wide range of Stark numbers and steady-state Biot numbers. The numerical scheme is computationally efficient and yields stable solutions. Changes in the geometry alter the form of the kernel in the integral equation, but the general principles used should be applicable to solve nonlinear integral equations.

Nomenclature

A = dimensionless relaxation time constant, $\gamma R^2/\alpha$
a_m = coefficients in Fourier series
Bi = Biot number, hR/λ
E = Stark number, $\varepsilon\sigma T_0^3 R/\lambda$
F = nondimensional generalized boundary condition
f, g = auxiliary functions in discretized integral equation
H = dimensionless initial time step
h = convection heat transfer coefficient, W m^{-2} K^{-1}
I_0, I_1 = modified Bessel functions
J_0, J_1 = Bessel functions of the first kind
j, k, l = indices in discretized equation
Pd = Predvoditelev criterion, $\beta R^2/\alpha$
Po = Pomerantsev criterion, $R^2 w_0 \lambda^{-1} T_0^{-1}$, $R^2 w_0 \lambda^{-1}(T_\infty - T_0)^{-1}$
R = radius of cylinder, m
r = radial coordinate, m
S = dimensionless source term
T = temperature, K
t = time, s
$W_{k,j}$ = weights for computing integral equation
w_0 = maximum specific strength of the source at $t = 0$, W m^{-3}
α = thermal diffusivity, m^2 s^{-1}
β = maximum relative rate of change of the dimensionless specific source strength
γ = relaxation time constant, s^{-1}
Δ_η = radial component of Laplace operator
ε = cylinder emissivity
ζ^n = heat transfer law for given boundary condition evaluated at previous times
η = dimensionless radial coordinate
θ = dimensionless temperature
Λ = fourth-order algebraic equation
λ_m, λ = eigenvalue, thermal conductivity, W m^{-1} K^{-1}
μ_n = eigenvalues of Bessel functions of the first kind of integer order one
ν = dummy variable in integral equation
Π = kernel of integral equation
ϕ = general function in integrand
σ = Stefan–Boltzmann constant, W m^{-2} K^{-4}
τ = dimensionless time
χ = noise function in integral equation
Ψ = generalized kernel of integral equation

Received Nov. 22, 1995; revision received April 26, 1996; accepted for publication May 28, 1996.
*Member of Technical Staff, Mechanical Engineering.
†Associate Professor, Department of Mathematics.

I. Introduction

IN science and engineering fields the description of physical phenomena is often formulated in terms of integral equations. The neutron transport theory, which yields the well-known Boltzmann equation in atomic physics, constitutes such a typical example. The momentum representation of the Schrodinger equation to the special case of a static interaction potential in ordinary space results in a homogeneous Fredholm integral equation. The formulation of heat transfer problems in terms of integral equations is another area that has potential advantages. For instance, the analysis of heat transfer problems by an integral method is easy to understand and lends itself to direct physical interpretation. One of the most attractive features of the integral method formulation is that the resulting solution would imply that the integral conservation of quantities is exactly satisfied over the whole calculation domain. When a heat exchange mechanism between a solid material and its environment involves conduction coupled with other heat transfer modes such as radiation[1] and convection,[2] non-

linear effects arise, and the solution of the energy equation by conventional finite difference methods may become cumbersome. If, in addition, the thermal process requires that a heat source term be taken into account to simulate the physics of a problem correctly, the incorporation of the source term into the discretized equations is not a trivial matter. The versatility of the integral equation (IE) approach, however, resides in the flexibility of treating the nonlinear boundary conditions and source terms without resorting to a linearization technique. The linearization procedure has become a common practice, as can be demonstrated by the widely used commercial codes implemented with semi-implicit algorithms.[3] The choice is made, not because it provides better results, but because the nominally linear framework would allow only a formally linear dependence, and the incorporation of linear dependence is better than treating the term as a constant.

Problems in which thermal radiation plus other modes of heat transfer occur simultaneously cannot be solved using presently available mathematical techniques. Except in the simplest cases, it is usually necessary to resort to numerical evaluation of the solutions. Thermal radiation is the most common heat transfer mode that occurs in specialized high technological applications, such as thermal sprays for rapid solidification of advanced materials,[4] liquid droplet radiators of spacecrafts,[5] and determination of thermophysical properties of spherical solid or liquid droplets levitated in outer space.[6] In the rarefied upper atmosphere, the effect of radiation becomes very significant indeed, and it becomes desirable to be able to predict the time variation of temperature. It is this time-dependent problem, as applied to a cylinder, that is considered in this work.

There is another class of problems for which the heat flux at the surface of a solid wall varies with time. In particular, in geothermal studies the heating (or cooling) of a rock adjacent to water flowing through a crevice experiences a heat transfer process in which the convective heat transfer coefficient varies as a function of time.[2] Becker et al.[2] simulate the heat exchange process by assuming that the rock is flat and long enough so that Cartesian coordinates can be used. In the present investigation, the boundary condition, for the cylindrical configuration, is allowed to vary not only as a function of temperature, but also with time.

The pioneering work of Chambre,[7] Abarbanel,[8] and Crosbie and Viskanta[9] set forth the foundations for the development of solutions to heat conduction problems formulated in terms of integral equations subject to nonlinear boundary conditions. The numerical schemes developed by Chambre[7] were based on successive approximations. Abarbanel[8] developed asymptotic expansions and proved that his solutions were consistent with results deduced from physical arguments. Crosbie and Viskanta[9] employed an alternate method of solution based on an approximation of the kernel by a separable kernel. These methods are limited to a restricted range of the independent variable. More refined analytical approximations[1] and numerical techniques[10-13] have surfaced in the literature with numerical stability and convergence properties subjected to the type of functions that appear outside of the integral sign. A number of numerical methods[2,14,15] have placed much emphasis on solving nonlinear Volterra equations with singular or well-behaved kernels, but not much consideration has been given to nonlinear convolution integrals with nonsingular kernels involving infinite series. The difficulty increases when the kernel is expressed in terms of Bessel functions, spherical functions, or some other special function. Furthermore, the inclusion of a heat sink places some restrictions on the stability of previous methods. In this study, an integral formulation of the heat conduction equation with a heat sink gives rise to a nonlinear Volterra integral equation of the second kind with a nonsingular kernel expressed in terms of an infinite series. In view of that, the main objective of this investigation is to apply a simple, but robust, newly developed multistep method for solving nonlinear integral equations. One advantage of the proposed linear multistep method is that larger initial time steps can be taken by introducing a mathematical artifice. Another relevant feature of the method is that boundary conditions and source terms are treated explicitly, avoiding the undesired traditional linearization process.

Two alternatives to solving heat conduction problems subject to nonlinear boundary conditions are used here as benchmarks. The first method is based on Fourier series expansions, and it is referred to as the pseudospectral method (PM). The general idea is taken from the published literature,[16] but a procedure of solution has been devised to obtain the solution in two steps, in analogous fashion to a superposition method. The second technique corresponds to a standard, implicit, finite difference calculation. The finite difference equation (FDE) technique is considered in the present analysis not only for its flexibility in solving the discretized governing energy equation, but also for studying its numerical efficiency relative to the integral method.

II. Formulation of the IE

A. Nonlinear Boundary Condition

The unsteady heat conduction equation[17] for an axisymmetric homogeneous cylinder with a continuous heat sink, initially at a uniform temperature, may be expressed using dimensionless variables as

$$\frac{\partial\theta}{\partial\tau}=\frac{1}{\eta}\frac{\partial}{\partial\eta}\left(\eta\frac{\partial\theta}{\partial\eta}\right)-S(\tau)=\Delta_\eta\theta-S(\tau) \tag{1}$$

Under the premise that the thermophysical properties of the medium are temperature-invariant, the transient radiative cooling is described by the dimensionless variables, $\theta = T/T_0$, $\eta = r/R$, and $\tau = \alpha t/R^2$. The analysis assumes that the heat transfer occurs in the radial direction only. The specific strength of the heat sink is assumed to obey an exponential law $S(\tau) = Po\cdot e^{-Pd\tau}$, and a power function of time $S(\tau) = Po(Pd\tau)^{1/2}$. In the Russian literature[17] Pd is known as the Predvoditelev criterion and is defined as $\beta R^2/\alpha$. The coefficient Po preceding the exponential function[17] is termed as the Pomerantsev criterion; in the present case $Po = R^2w_0\lambda^{-1}T_0^{-1}$. The cylinder has an initial temperature T_0 and the ambient is assumed to be at an absolute temperature of 0 deg.

The transient diffusion equation is subjected to the initial condition $\theta(\eta, 0) = 1$. The symmetry condition requires that $\theta'(0, \tau) = 0$. The boundary condition at the surface of the cylinder may be conveniently written as $\theta'(1, \tau) = -F[\theta(1, \tau)]$. Specifically, the radiation condition $F = E\theta_s^4$ is used to quantify the heat losses from the cylinder surface during the transient radiative cooling. For the linear case, one simply takes $F = Bi\theta_s$. The subscript s stands for surface temperature. The constants of proportionality are known as the Stark number[17] $E = \varepsilon\sigma T_0^3R/\lambda$, and the Biot number $Bi = hR/\lambda$. The surface of the cylinder is gray with a total emissivity ε taken as a constant. The radiation shape factor between the surface of the cylinder and the sink is one. The nonlinear integral equation is obtained by applying the Laplace transform to Eq. (1) and the convolution theorem (see Appendix) to yield

$$\theta(\eta,\tau)=1+\chi(\tau)-2\int_0^\tau F[\theta_s(\nu)]\Pi(\eta,\tau-\nu)\,d\nu \tag{2}$$

The source functions, where $\chi(\tau) = -(Po/Pd)(1 - e^{-Pd\tau})$ or $\chi(\tau) = -(2/3)Po(Pd\tau^3)^{1/2}$, and the infinite series kernel given by $\Pi(\eta, \tau - \nu) = 1 + \Sigma_{n=1}^{\infty} J_0(\mu_n\eta)J_0(\mu_n)^{-1}\exp[-(\tau - \nu)\mu_n^2]$ have been used. J_0 represents the Bessel function of the first kind of integer order zero where the μ_n are the roots of $J_1(\mu_n) = 0$.

B. Time-Dependent Boundary Condition

This section considers that $T_0 > T_\infty$, where T_∞ is now the ambient temperature. The dimensionless temperature is des-

ignated by $\theta = (T - T_0)/(T_\infty - T_0)$. As a consequence of this definition the initial condition now becomes $\theta(\eta, 0) = 0$, whereas the symmetry condition remains unchanged. Consequently, the Pomerantsev criterion acquires a slightly different form since the ambient temperature is different from zero, i.e., $Po = R^2 w_0 \lambda^{-1}(T_\infty - T_0)^{-1}$. However, the Predvoditelev criterion does not suffer any modification. The approximation suggested by Becker et al.[2] for the convective heat transfer coefficient is chosen in this study. The convective heat transfer coefficient in physical space is expressed as $h = h_0(1 - e^{-\gamma t})$. In this equation h_0 is the steady-state heat transfer coefficient. At the solid surface the heat flux may be written as $\theta'(1, \tau) = -Bi_0(1 - e^{-A\tau})[\theta(1, \tau) - 1]$. The procedure for deriving the nonlinear integral equation with a time-dependent boundary condition is obtained similarly as for the Stefan–Boltzmann radiating case. The cylinder temperature distribution in the form of a Volterra convolution integral equation (see Appendix) is given by

$$\theta(\tau, \eta) = \chi(\tau) - 2Bi_0 \int_0^\tau (1 - e^{-A\nu})[\theta_s(\nu) - 1]\Pi(\eta, \tau - \nu)\, d\nu \tag{3}$$

In Eq. (3) the functions $\chi(\tau)$, and $\Pi(\eta, \tau - \nu)$ are described in Sec. II.A. The constant A is defined as $\gamma R^2/\alpha$. It can be shown that when $A \to \infty$ and T_∞ is set equal to zero, the time-dependent boundary condition reduces to the linear case [see Eq. (2)]. One can readily see that the desired surface temperature is simply found by setting $\eta = 1$ in Eqs. (2) and (3). Since the kernel of the integral equation depends on the chosen geometry, the IE in Eq. (3) is not the same as that solved by Becker et al.[2] in Cartesian coordinates.

III. Numerical Solution

A. Integral Equation Method

The numerical method for solving the nonlinear Volterra equation of the second kind is discussed next. It is convenient to express Eqs. (2) and (3) in a suitable form for numerical treatment. Hence, the convolution integral equations in the interval $[0, \tau]$ may be written generally as

$$f(\tau) - \int_0^\tau \Psi(\tau, \nu, F[f(\nu)])\, d\nu = g(\tau) \tag{4}$$

The existence of a unique solution to this nonlinear equation is required. It is plausible to assume for the moment that $\Psi(\tau, \nu, F[f(\nu)])$ and $g(\tau)$ are smooth functions. By the use of the linear multistep method,[10,18,19] the solution of the Volterra equation is obtained by writing down Eq. (4) in a sequence of equidistant points, $\tau_j = \tau_0 + jH$. Thus, the integral can be approximated by adapting the idea of the quadrature rule,[20] leading to a discrete convolution integral

$$\int_0^{kH} \phi(\nu)\, d\nu \approx \sum_{j=0}^{k} W_{k,j}\phi(jH) \tag{5}$$

The weights $W_{k,j}$ are defined next. The quadrature rule provides an equation

$$\tilde{f}(kH) - \sum_{j=0}^{k} W_{k,j}\Psi(kH, jH, F[\tilde{f}(jH)]) = g(kH) \tag{6}$$

with $k = 0, 1, 2, \ldots$. The trapezoid rule fails to give good accuracy and it is not recommended unless $\Psi = \Psi(\tau, \nu, F[f(0)])$. This does not apply here and the integration procedure requires another alternative. From the point of view of the local truncation error, Simpson's one-third rule is to be preferred. However, in the procedure of computing the solution for the temperature distribution, k takes even as well as odd values, and a modification is necessary since the repeated version of Simpson's one-third rule is used only when k is even. As a result, a repeated version of Simpson's one-third rule together with Simpson's three-eighths rule is used when k is odd.[21] This alternating combination generates the set of weights that are needed to carry out the integration. When the integer k takes on even values, Eq. (5) becomes

$$\int_0^{2lH} \phi(\nu)\, d\nu = \frac{H}{3}[\phi(0) + \phi(2lH)] + \frac{2H}{3}\sum_{j=1}^{l-1} \phi(2jH) + \frac{4H}{3}\sum_{j=0}^{l-1} \phi(2jH + H) \tag{7}$$

and for k odd, it is recommended to write[21]

$$\int_0^{(2l+1)H} \phi(\nu)\, d\nu = \int_0^{(2l-2)H} \phi(\nu)\, d\nu + \int_{(2l-2)H}^{(2l+1)H} \phi(\nu)\, d\nu \tag{8}$$

with $l = 1, 2, \ldots$. Note that this scheme breaks up the integration time domain in two well-defined sets of panels. The first set of panels corresponding to the integration interval $0 \to (2l - 2)H$ yields an even number of subintervals. Thus, the first integral on the right-hand side (RHS) of Eq. (8) is approximated by Simpson's one-third rule, as was used earlier for the case when k is even. The second time range, $(2l - 2)H \to (2l + 1)H$, which always has three panels, suggests the use of Simpson's three-eighths rule. The weights for Simpson's three-eighths rule are extracted from the ϕ coefficients on the RHS of the expression given by

$$\int_{(2l-2)H}^{(2l+1)H} \phi(\nu)\, d\nu = \frac{3H}{8}\phi[(2l - 2)H] + \frac{9H}{8}\phi[(2l - 1)H] + \frac{9H}{8}\phi[2lH] + \frac{3H}{8}\phi[(2l + 1)H] \tag{9}$$

Hence, for k odd, the global error is reduced by combining the two integration rules. The method is stable and its rate of convergence is proportional to H^4. It has been found that the one-third and three-eighth rules yield the best accuracy. The only requirement is that the three-eighths rule has to be applied in that interval for which the fourth derivative of the function is smallest.

As the time variable increases, a new set of weights has to be determined, so that the solution can proceed in a step-by-step fashion. A condition satisfied by Eq. (6) is that $f(0) = g(0)$. Then, if $f(H), f(2H), \ldots, f[(l - 1)H]$, have been found in sequence, one gets the equation

$$\tilde{f}(kH) - W_{k,k}\Psi(kH, kH, F[\tilde{f}(kH)]) = g(kH) + \sum_{j=0}^{k-1} W_{k,j}\Psi(kH, jH, F[\tilde{f}(jH)]) \tag{10}$$

The linear multistep scheme has converted the nonlinear integral equation into a sequence of nonlinear algebraic equations with a single unknown, which represented in compact form gives $\Lambda[\tilde{f}(lH)] = 0$. The order of the equation for Λ depends on the kind of boundary condition. For example, the Stefan–Boltzmann boundary condition gives rise to a fourth-order algebraic equation. Solving this equation yields the surface temperature at each step. The real zeros of the continuous function are found by the secant method.

Often the question arises as to whether the qualitative behavior of the discretized equation reflects that of the original problem. Lubich[11] and Amini[12] have analyzed this question and

the stability problem. Lubich points out that the linear multistep method for linear integral equations is stable, provided that $f(\tau)$ remains bounded whenever $g(\tau)$ is bounded. On the other hand, Amini[12] extends his analysis to include the nonlinear convolution integral and establishes that uniform boundedness of the differential resolvent is necessary and sufficient for uniform stability assuming sufficient smoothness in Ψ and $g(\tau)$. Since the surface temperature distribution of a convecting or radiating object obeys a monotone decreasing (or increasing) function, and the previous implications are met, the method is guaranteed to be stable over the entire time domain.

B. PM

The temporal term in Eq. (1) is approximated by the usual forward difference formula such that $(\theta^{n+1} - \theta^n)/\Delta\tau = \Delta_\eta\theta^{n+1} + S^{n+1/2}(\tau)$. When this equation is multiplied by $\Delta\tau$ and solved for θ^{n+1}, the following expression results:

$$(\Delta\tau\cdot\Delta_\eta - 1)\theta^{n+1} + \bar{S}(\tau)^{n+1/2} = 0 \tag{11}$$

The second term on the left-hand side of Eq. (11) consists of two known contributions, $\bar{S}^{n+1/2} = \theta^n + \Delta\tau\cdot S^{n+1/2}$, where $S^{n+1/2} = (S^{n+1} + S^n)/2$. With the previous discretization procedure for the heat conduction equation, the partial differential equation collapses into a nonhomogeneous differential equation subject to a general nonlinear boundary condition denoted as $(\theta')^{n+1}(1, \tau) = \zeta^n$. The solution to Eq. (11) proceeds in two steps. In the first step the homogeneous problem is considered imposing the nonhomogeneous boundary condition. In the second step the nonhomogeneous differential equation is solved subject to a homogeneous boundary condition.

For the first step, Eq. (11) simplifies to $\Delta\tau\cdot\Delta_\eta\theta^{n+1} - \theta^{n+1} = 0$, subject to $(\theta')^{n+1}(1, \tau) = \zeta^n$. The particular solution happens to be given by

$$\theta_I^{n+1}(\eta) = \zeta^n\sqrt{\Delta\tau}\,\frac{I_0(\eta/\sqrt{\Delta\tau})}{I_1(1/\sqrt{\Delta\tau})} \tag{12}$$

The evaluation of the modified Bessel functions (I_0, I_1) of integer orders zero and one is discussed in section four. The second solution requires that Eq. (11) be solved along with a homogeneous side condition. Assuming that $\bar{S}^{n+1/2}$ in Eq. (11) can be expanded into a Fourier series, the problem can be stated by considering an eigenvalue problem instead. That is to say, the solution to the problem

$$(\Delta\tau\cdot\Delta_\eta - 1)\theta_{II}^{n+1} + \lambda\theta_{II}^{n+1} = 0 \tag{13}$$

is sought, subject to $(\theta_{II}')^{n+1} = 0$. The eigenfunctions are given by $\theta_{II}^{n+1} = C_m J_0(\kappa_m\eta)$, and the eigenvalues satisfy the equality $J_1(\kappa_m) = 0$, where $\kappa_m = \sqrt{(\lambda_m - 1)/\Delta\tau}$. Then, the second solution is represented as a Fourier series, $\theta_{II}^{n+1}(\eta) = \sum_{m=1}^{\infty} a_m J_0(\kappa_m\eta)$, such that it satisfies Eq. (11). Analogously, it is also valid to write $\bar{S} = \sum_{m=1}^{\infty}\bar{S}_m J_0(\kappa_m\eta)$. Hereafter, the superscript $(n + 1/2)$ is dropped from $\bar{S}(\tau)$ and $\bar{S}_m(\tau)$. What is needed now is to know how a_m is related to $\bar{S}_m$. To derive the relationship between the two coefficients, the Fourier series for θ_{II}^{n+1} and for $\bar{S}$ are substituted into Eq. (11) to get

$$\sum_{m=1}^{\infty}[a_m(\Delta\tau\cdot\Delta_\eta - 1)J_0(\kappa_m\eta) + \bar{S}_m J_0(\kappa_m\eta)] = 0 \tag{14}$$

Recalling that $\theta_{II}^{n+1} = C_m J_0(\kappa_m\eta)$ are the eigenfunctions of the eigenvalue problem for Eq. (13), then Eq. (13) can be cast in the form $(\Delta\tau\cdot\Delta_\eta - 1)J_0(\kappa_m\eta) = -\lambda_m J_0(\kappa_m\eta)$. When this equation is substituted into Eq. (14) the desired relationship for the Fourier series coefficients is obtained. Hence, the coefficients a_m for the Fourier series of θ_{II}^{n+1} are related to the coefficients $\bar{S}_m$ through the equality $-\lambda_m a_m + \bar{S}_m = 0$, for $m = 0, 1, 2, \ldots, \infty$. As a result, the second solution expressed as a Fourier series is given by

$$\theta_{II}^{n+1}(\eta) = \sum_{m=1}^{\infty}\frac{\bar{S}_m}{\lambda_m}J_0(\kappa_m\eta), \qquad \kappa_m = \sqrt{(\lambda_m - 1)/\Delta\tau} \tag{15}$$

The complete solution is, therefore, $\theta^{n+1} = \theta_I^{n+1} + \theta_{II}^{n+1}$. One has to keep in mind that $\bar{S}$ and ζ are evaluated at the layer (n). Since λ_m is calculated from the zeros of $J_1(\kappa_m)$, it is left to determine the coefficients $\bar{S}_m$. This is a straightforward technique using the orthogonality of eigenfunctions, thus,

$$\bar{S}_m = \frac{2}{[J_0(\kappa_m)]^2}\int_0^1 \bar{S}(\eta)\eta J_0(\kappa_m\eta)\,d\eta \tag{16}$$

C. FDE Method

To find the transient temperature distribution, Eq. (1) must be finite differenced and numerically evaluated. The spatial derivative in Eq. (1) is finite differenced by using standard central difference techniques while the time derivative is discretized with a forward finite difference equation. To eliminate stability problems in the evaluation of temperature, an implicit scheme is adopted. The complete details of the finite difference formulation of the transient conduction equation is documented in the literature.[22] Combining the finite difference form of the temporal and diffusion terms of the heat conduction equation yields a tridiagonal system of equations that can be put in the following form: $A_i\theta_{i-1}^{k+1} + B_i\theta_i^{k+1} + C_i\theta_{i+1}^{k+1} = D_i^k$. In this equation, the current time index is denoted as k, and the subsequent time index for which θ is being solved is $k + 1$. The RHS vector $D_i^k = -\theta_i^k + Po\Delta\tau e^{-Pd\tau^k}$ is evaluated at the current time. Of great importance in the temperature evaluation is the incorporation of the boundary conditions into the tridiagonal coefficient matrix of the interior node points. At the center of the cylinder, $A_1 = 0$, the tridiagonal form of the equation can be written as

$$-\left(1 + \frac{4}{\eta_2^2}\Delta\tau\right)\theta_1^{k+1} + \frac{4\Delta\tau}{\eta_2^2}\theta_2^{k+1} = -\theta_1^k + Po\Delta\tau e^{-Pd\tau^k} \tag{17}$$

At the surface of the cylinder it is required that $C_N = 0$, resulting in the tridiagonal system

$$\frac{\Delta\tau(1 + \eta_{N-1}/\eta_N)}{(\eta_N - \eta_{N-1})}\theta_{N-1}^{k+1} - \left[1 + \frac{2\Delta\tau\mathcal{T}(\theta)_N^k}{(\eta_N - \eta_{N-1})} + \frac{\Delta\tau(1 + \eta_{N-1}/\eta_N)}{(\eta_N - \eta_{N-1})^2}\right]\theta_N^{k+1} = -\theta_N^k + Po\Delta\tau e^{-Pd\tau^k} \tag{18}$$

The function $\mathcal{T}(\theta)_N^k$, in Eq. (18), is equal to $E\theta^3|_N^k$ for the Stefan–Boltzmann boundary condition, and is identical to Bi for the linear side condition. When the heat exchange at the surface obeys the time-dependent Newton's cooling law, then $\mathcal{T}(\theta)_N^k = Bi_0(1 - e^{-A\tau})$. This kind of boundary modifies the RHS independent vector with an additional contribution that sums up to yield

$$D_i^k = -\theta_i^k + Po\Delta\tau e^{-Pd\tau^k} - 2\Delta\tau Bi_0(1 - e^{-A\tau^k})/(\eta_N - \eta_{N-1})$$

IV. Results

Before going into the details of the numerical evaluation of the integral equations, it is important to mention how the computation is initialized. Because of the rapid variation of θ_s for small τ, it is crucial to get a few values of θ_s for small τ. Asymptotic expansions for small values of the independent variable were derived for the two cases studied here. In what follows case 1 means the Stefan–Boltzmann boundary condition, and case 2 refers to the time-dependent side condition. For case 1 two kinds of heat sinks are considered. One heat

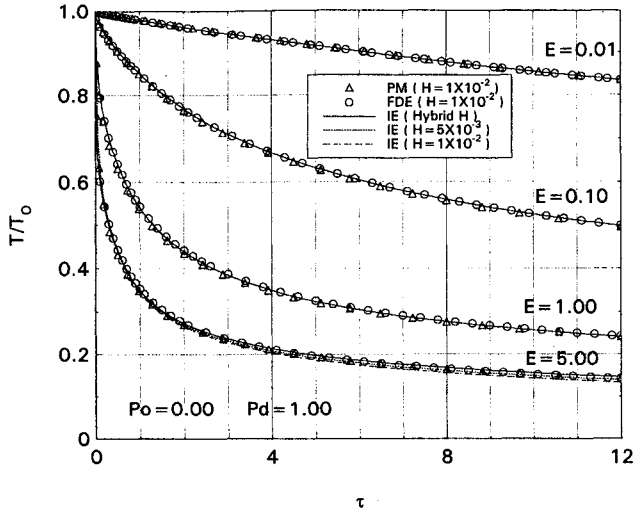

Fig. 1 Normalized surface temperature distributions of a radiating cylinder without a heat sink.

source changes by an exponential law, $\chi(\tau) = -PoPd^{-1}(1 - e^{-Pd\tau})$, and the other as some power function of time, $\chi(\tau) = -(2/3)Po(Pd\tau^3)^{1/2}$. The formula $\theta_s(\tau) = 1 + \chi(\tau) - 2E\sqrt{\tau/\pi}$ is used to determine the initial surface temperature for case 1, whereas the following two-term equation, $\theta_s(\tau) = \chi(\tau) + 1.334A \cdot Bi_0\tau\sqrt{\tau/\pi}$, supplies the transient temperature values for case 2. These two expressions are easy to get. Consider the Stefan–Boltzmann boundary condition; one can see that near $\tau \approx 0$, $F = E\theta_s^4 \approx E$. Then, taking the limit as $s \to \infty$ in Eq. (A3), and subsequent application of the inversion theorem, gives the desired expression. Typically, five temperature values are sufficient to start the numerical computation.

The numerical results for case 1 without a heat sink are shown in Fig. 1. The omission of the source term has been made with the sole purpose of comparing the predictions with an asymptotic expansion formula for large τ, derived using standard techniques. The comparison is discussed later. The mathematical analysis to obtain the asymptotic expansion is not given in this article, but the interested reader can find the details for the sphere problem in Ref. 7. Figure 1 compares the IE numerical calculations with the PM and the FDE solutions for four radiation numbers (0.01, 0.1, 1.0, and 5.0). The IE temperature profiles are obtained with an initial time step $H = 0.01$. Both the FDE and PM schemes, with 40 grid points uniformly spaced along the radial coordinate, employ the same initial time step. For Stark numbers, 0.01, 0.1, and 1.0, the IE approach requires an average of 1.5 s of CPU time on an Alpha workstation. The FDE numerical method, on the other hand, takes approximately a CPU time of 1.0 s on the same computer. The CPU time for the PM is addressed later.

The heat transfer rate at the surface of the cylinder changes drastically for small τ as the radiation number becomes larger. The initial time step is a critical parameter in the initial stages of the computation. Although the integral method has been demonstrated to be numerically stable and to possess good convergence properties for $H = 0.01$, it can be seen from Eq. (9) that as the initial step is reduced by a fraction of the original H, the computing time is increased accordingly. This may hinder the numerical efficiency of the multistep method for large radiation parameters. For example, the numerical solution from $\tau = 0$ to 12 takes about 6 s on an Alpha computer with $E = 1.0$ and $H = 0.005$. A shortcut is devised to avoid computationally expensive runs for large E due to a small H. The solution is found in a two-phase sequence. First, the code is run for a given E with a very small H to a specified τ that is sufficiently large ($\tau \leq 0.07$). Second, within the prescribed time range ($0 < \tau \leq 0.07$), five to six computed temperature values that are selected arbitrarily, but taken at uniform intervals based on an H that is a multiple of the original H of the first phase, are chosen. Then, the code is run again for the new H. In this form the complete temperature distribution is obtained. Following this procedure the code takes only 2.0 s to run on a workstation with $E = 5.0$ ($H_1 = 0.001$, $\tau_1 = 0.07$; $H_2 = 0.01$, $\tau_2 = 12$) and reproduces the solid curve shown in Fig. 1. The other two curves shown by dashed lines are found in the usual way. The farthest curve from the solid line is obtained with $H_1 = 0.01$, and the dashed line in between is determined with a value of $H_1 = 0.005$. A quick calculation using the asymptotic formula for large times, $\theta_s = T/T_0 = 1/\sqrt[3]{6E\tau}$, reveals that the IE, FDE, and the PM numerical solutions tend to the asymptotic value $T/T_0 = 0.52$, 0.24, and 0.14 for $E = 0.1$, 1.0, and 5.0 at $\tau = 12$. The asymptotic formula fails for $E = 0.01$ since the solution has not yet reached steady state. This confirms the validity of such results and gives enough confidence in the present method to handle nonlinear boundary conditions.

The Bessel functions and the modified Bessel functions needed for the PM calculation are evaluated directly by means of numerical approximations,[20] and the numerical integration of Eq. (16) is performed with a Gaussian integration formula.[20] Normally, an average of 18 s of CPU time on an Alpha workstation is sufficient to get the desired temperature profile for each radiation number.

Figure 2 shows the surface temperature results for the radiating cylinder with an exponential heat sink taking $Po = 0.50$ and $Pd = 1.00$. Again, the calculations are executed for four radiation numbers (0.01, 0.1, 1.0, and 5.0). The FDE and PM solutions are performed with $\Delta\tau = 0.005$ and with the same number of grid points that have been used in the previous case. The integral method uses also the same initial time step. The reason for choosing H as half of the value that is used to generate most of the results in Fig. 1 is twofold. First of all, it is convenient to eliminate the mathematical artifice adopted for finding the predicted temperature distribution in two strokes and to observe how the method responds. Secondly, the numerical efficiency of each numerical approach needs to be evaluated. In regard to the first question it can be seen from Fig. 2 that there is a remarkable agreement between the IE predictions with the FDE and PM solutions. The second question is answered by comparing the corresponding CPU times of the three methods using $H = 0.005$. The following CPU time ratios are found: $IE_{CPU}/FDE_{CPU} \approx 3$, whereas $IE_{CPU}/PM_{CPU} \approx 0.2$. What the first ratio implies is that the FDE formulation tends to be computationally more efficient as H is reduced. On the contrary, a reverse trend occurs between the IE and PM

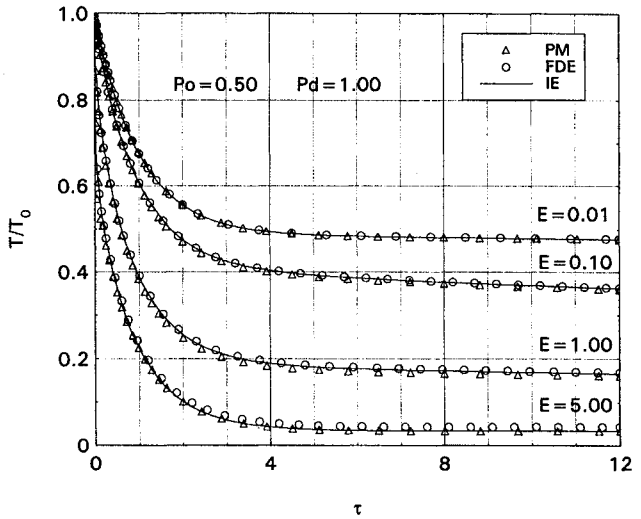

Fig. 2 Normalized surface temperature distributions of a radiating cylinder with a heat sink that changes exponentially with time.

methods. At this point it is interesting to analyze the opposite effect, that is, how effective the three methods are in predicting the transient temperature as H is increased, say, by approximately five times its value ($H = 0.025$). Surprisingly, what is found is that $IE_{CPU}/FDE_{CPU} \approx 0.6$, and $IE_{CPU}/PM_{CPU} \approx 0.08$. This means that for greater H values the IE is better than the FDE scheme, but the PM method becomes even less efficient.

The performance of the numerical integral method for handling kernels expressed in terms of infinite series that contain Bessel functions is evaluated next. The Bessel function of integer order zero is evaluated by two polynomial approximations[20] defined in the intervals: $-3 \leq \eta \leq 3$ and $3 \leq \eta < \infty$. Figure 3 presents the internal and surface temperature profiles for a cylinder with $E = 0.70$ and a heat source that varies exponentially with time. The Predvoditelev and Pomerantsev coefficients are 1.0 and 0.10, respectively. To eliminate the crowding of data points only two spatial locations inside the cylinder are plotted. In all runs the three numerical algorithms employ 0.005 as the initial time step. Even though Fig. 3 shows a time range from zero to three, the integration is carried out until the dimensionless time reaches a magnitude of 12 units. At $\tau \approx 3$ the internal temperature distributions are almost attained the outside surface temperature. Beyond $\tau = 4$ all curves collapsed into a single curve.

The accuracy and robustness of the present method for solving Volterra equations of the second kind are verified by considering another source term variation. The trivial choice, that is, a constant heat sink, is excluded here since this situation does not pose any serious threat to the stability of the method. The second and most important selection is to assume that the source term is proportional to a power function of time. In other words the heat sink is mathematically represented by $S(\tau) = Po(Pd\tau)^{1/2}$. When the source term is inserted into Eq. (1) and the corresponding integration performed, it results that the noise function in Eq. (3) is given by $\chi(\tau) = -(2/3)Po(Pd\tau^3)^{1/2}$. The transient temperature for various Stark numbers is computed using the three working numerical schemes for $Po = 0.01$ and $Pd = 0.05$. The numerical predictions computed with $H = 0.005$ are graphically represented in Fig. 4 for a range of Stark numbers of physical interest. Here again, the agreement between the IE method with the FDE and PM approaches is excellent. Also Fig. 4 displays the surface temperature of the cylinder that has Po and Pd as 0.5 and 1.0, respectively, for $E = 0.01$. The purpose of generating this distribution is to observe how the solutions for the two types of source terms (Figs. 2 and 4) behave. The drastic decay of the surface temperature toward zero happens in the time interval (0, 2) when the heat sink obeys a power dependence on time. The solution for a source term that changes exponentially with time reaches an asymptotic temperature value [$\theta_s(1, \tau) \rightarrow 0.47$] soon after the cylinder cools down to 0 deg when the source term changes as a power function of time. Evidently, the strength of the heat source that changes as some power function of time tends to accelerate the cooling process under the same given conditions.

The numerical calculations for case 2 are shown in Figs. 5 and 6 for a specific strength of a heat source that is governed by an exponential law. All three schemes use $H = 0.01$ as the initial time step. In Fig. 5 the predicted temperature profiles at the cylinder boundary are depicted for three steady-state Biot numbers (5.0, 1.0, and 0.5). As the Biot number decreases a discrepancy becomes apparent between the PM method with respect to both the IE and FDE methods. The inconsistency is accentuated for the curve corresponding to $Bi_0 = 0.5$. Since the IE and FDE formulations are more sensitive to the initial time step, it happens that these two methods cannot resolve with a high degree of accuracy the decay in the cylinder's temperature for small times, unless a very small time step is taken; the system of equations becomes stiff as $Bi_0 \rightarrow 0$. For smaller H the divergence starts to vanish as will be seen in the next

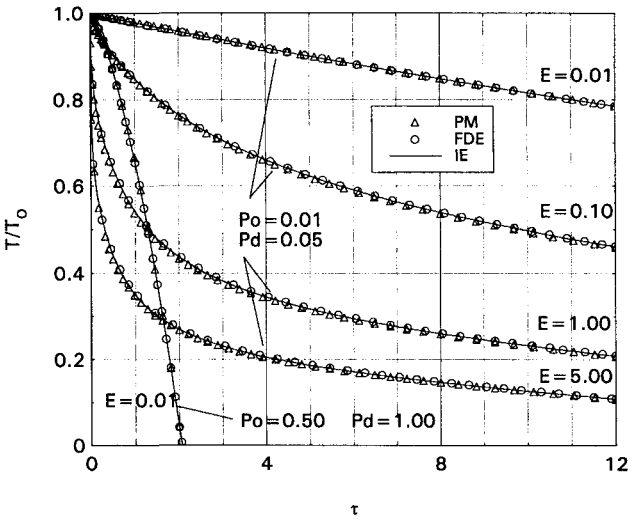

Fig. 4 Normalized surface temperature distribution of a radiating cylinder with a heat sink that obeys a power dependence on time.

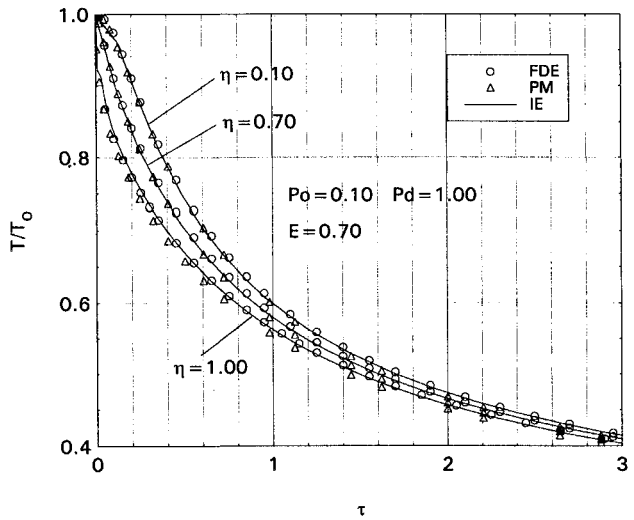

Fig. 3 Normalized internal and surface temperature distribution of a radiating cylinder with a heat sink that changes exponentially with time.

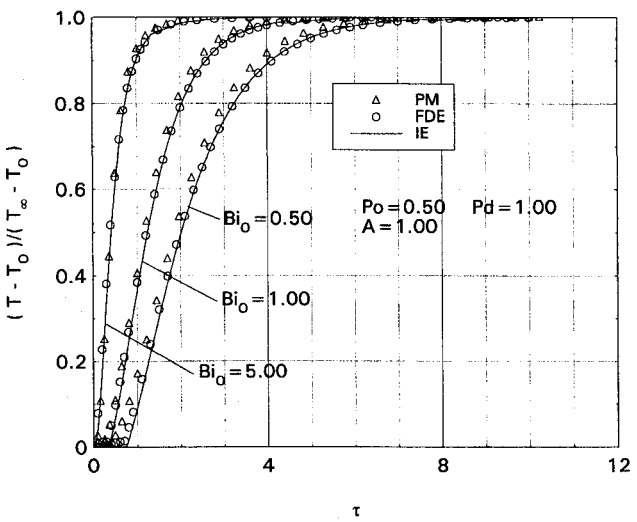

Fig. 5 Normalized surface temperature distribution of a time-dependent convective cylinder with a heat sink that changes exponentially with time.

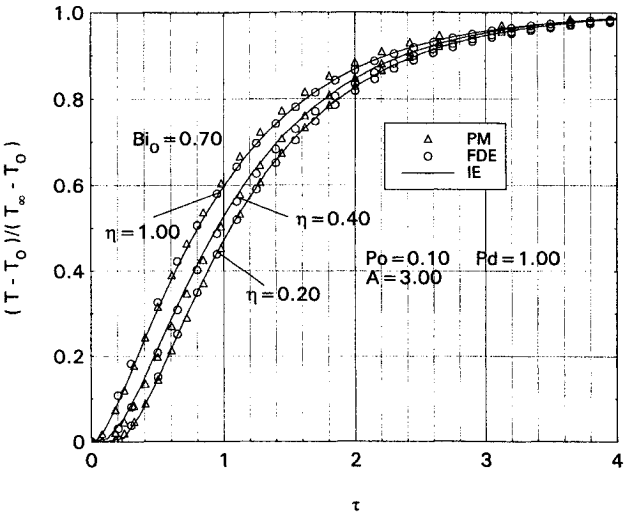

Fig. 6 Normalized internal and surface temperature distribution of a time-dependent convective cylinder with a heat sink that changes exponentially with time.

figure. The CPU time ratios, IE_{CPU}/FDE_{CPU} and IE_{CPU}/PM_{CPU}, are comparable to those of the radiating cylinder. The temperature history inside the cylinder has been computed at two spatial locations. Figure 6 shows the thermal variation of a cylinder with a steady-state Biot number equal to 0.70, a relaxation time constant of 3, and $Po = 0.10$ and $Pd = 1.0$. In general, the comparison between the IE technique with the other two mathematical schemes is acceptable. The chosen time step used to run the code is taken to be half of what is used in the previous situation, that is, 0.005. Although the temperature range that was actually covered was from 0 to 12, Fig. 6 only shows the internal temperature distribution in the first stage where temperature gradients prevail. The entire transient cylinder's temperature becomes identical as the time approaches 4.

V. Conclusions

In summary, the use of the linear multistep method based on a composite formula works very well over the entire time range for both cases 1 and 2. The numerical approach is numerically stable and computationally efficient. The asymptotic expansion for large τ ensures that the solution is converged to the correct steady-state temperature when there is no heat source. When the user desires to take a larger step size (i.e., $H > 0.005$), the two-phase sequence is found to give acceptable results, even if the kernel of the integral equation becomes stiff ($E > 1$ and $Bi < 1$). The mathematical artifice can be avoided at the cost of choosing a smaller initial time step. The numerical solutions produced with the IE scheme agree reasonably well with both the FDE and PM predictions in the time range covered. In the present study the FDE and PM methods are shown to be satisfactory, but rather wasteful because much unneeded information concerning the internal cylinder temperature must be obtained. The finite difference technique appears to be more efficient than the integral method as the initial time step is decreased, but an opposite trend occurs as H increases. In both instances the PM method turned out to be less efficient than the IE scheme. The accuracy/robustness of the integral method is proved by testing two kinds of heat sources, an exponential law and a power function of time. Inside temperature profiles have been obtained for cases 1 and 2. A wider variety of dimensionless numbers have been tested, given in all circumstances stable solutions.

Writing standard programs using routines for $F[\theta_s]$ and $\Pi(\eta, \tau)$ as arguments, would make the integral equation approach easier to use. Different geometries should be investigated. Changes in the geometry alter the form of the kernel in the integral equation, but the general principles used should be applicable. To apply the basic idea to practical problems, the integral equation for the surface temperature must be generalized to multidimensional cases involving integration over multiple space dimensions in addition to time. Obviously, this is much more difficult. However, as the dimensionality is lowered more than for the original problem, there should be considerable savings once standard programs are developed.

Generalizing the physical problem to include factors such as nonuniform initial temperature, nonconstant material properties, and the presence of a surrounding medium, would be a long range goal that would involve considerable difficulty. The original problem would no longer be linear, and so it would be difficult to set up the kernel of the integral equation as an analytical expression.

It is important to keep in mind that, with the recent advances in numerical analysis and the explosive developments of computational devices of all types, it is a straightforward task to carry out two- or three-dimensional simulations, which include full radiation effects, by direct application of finite volume techniques or a similar numerical tool. Nonetheless, it is important not to forget that these simulations regrettably rely on linearization techniques for both source terms and nonlinear boundary conditions. It is well known that an incorrect linearization of the source term may lead to a nonconverging solution. Furthermore, unless the numerical method is fully implicit, there is always the possibility that numerical instability will be present. The majority of the available commercial codes, if not all, use underrelaxation techniques since the governing equations are solved sequentially. It would be pertinent to examine the behavior between an integral equation approach and a finite difference scheme for the unsteady, multidimensional energy equation, subjected to nonlinear boundary conditions before a final conclusion can be reached.

Appendix: Volterra Integral Equations

This section presents the derivation of the nonlinear Volterra equations of the second kind for the two study cases. The Stefan–Boltzmann boundary condition is treated first assuming that the source term changes exponentially with time. Application of the Laplace transform to Eq. (1) yields

$$\eta \frac{d^2\bar{\theta}}{d\eta^2} + \frac{d\bar{\theta}}{d\eta} - s\eta\bar{\theta} = -\eta + \frac{Po}{s + Pd}\eta \qquad \text{(A1)}$$

where $l\{\theta(\eta, \tau)\} = \bar{\theta}(\eta, s)$. Initial and boundary conditions are stated in Secs. II.A and II.B, respectively. The general solution to this linear, nonhomogeneous, second-order differential equation is given by

$$\bar{\theta} = \frac{1}{s} - \frac{Po}{s(s + Pd)} + C_1 J_0(i\eta\sqrt{s}) \qquad \text{(A2)}$$

The constant of integration C_1 is determined by combining the Stefan–Boltzmann boundary condition with Eq. (A2). Doing the algebraic work, the particular solution turns out to be

$$\bar{\theta}(\eta, s) = \frac{1}{s} - \frac{Po}{s(s + Pd)} - \frac{\bar{F} I_0(\eta\sqrt{s})}{\sqrt{s} I_1(\sqrt{s})} \qquad \text{(A3)}$$

Here the recurrence relationship $I_n(x) = i^{-n} J_n(xi)$ was used. Now the convolution theorem given by

$$l\left\{\int_0^\tau G(\tau - \nu)F(\nu)\, d\nu\right\} = \bar{F}(s)\bar{G}(s) \qquad \text{(A4)}$$

is used to invert Eq. (A3). The two Laplace transforms of $\bar{F}$ and $\bar{G}$ are chosen as

$$\bar{G}(s) = \frac{I_0(\eta\sqrt{s})}{\sqrt{s}I_1(\sqrt{s})}, \qquad \bar{F}(s) = El\{F\} \tag{A5}$$

The recovery of $G(\tau)$ follows from the inversion theorem, stated as

$$G(\tau) = \frac{1}{2\pi i}\int_{\gamma+i\infty}^{\gamma+i\infty} \frac{\exp(z\tau)I_0(\eta\sqrt{z})}{\sqrt{z}I_1(\sqrt{z})}\,dz \tag{A6}$$

Notice that the presence of $(z)^{1/2}$ in the denominator of Eq. (A6) might lead us to believe that $z = 0$ is a branch point. By expanding the integrand of Eq. (A6) relegating the exponential function, it yields

$$\frac{I_0(\sqrt{z}\eta)}{\sqrt{z}I_1(\sqrt{z})} = \frac{1 + z\eta^2/2^2 + z^2\eta^4/(2^2 4^2) + \cdots}{z/2 + z^2/(2^2 4) + \cdots} \tag{A7}$$

The polynomial in the denominator shows clearly the absence of a branch point at $z = 0$. Nonetheless, a simple pole exists at $z = 0$. Next, the full argument of the integrand in Eq. (A6) is expanded as

$$\frac{\exp(z\tau)I_0(\sqrt{z}\eta)}{\sqrt{z}I_1(\sqrt{z})} = \frac{(1 + \tau z + \cdots)[1 + z\eta^2/2^2 + z^2\eta^4/(2^2 4^2) + \cdots]}{z/2 + z^2/(2^2 4) + \cdots} \tag{A8}$$

for finding the residue at $z = 0$. Now, Cauchy's residue theorem

$$\mathcal{R}_a = \frac{1}{(k-1)!}\left[\frac{d^{k-1}}{dz^{k-1}}(z-a)^k f(z)\right]_{z=a} \tag{A9}$$

supplies the single pole. Taking $a = 0$ and $k = 1$, one obtains $\mathcal{R}_0 = 2$. Besides the single pole, $G(s)$ has an infinite number of poles at $z = -\mu_n^2$. Those can be directly evaluated from the generalized polynomials in Laplace's domain

$$\sum_{n=1}^{\infty} \mathcal{R}_{-\mu_n^2} = \sum_{n=1}^{\infty} \frac{P(-\mu_n^2)}{Q(-\mu_n^2)\left(\frac{dR}{dz}\right)_{z=-\mu_n^2}} \tag{A10}$$

Setting $P = \exp(z\tau)I_0(\eta\sqrt{z})$, $Q = \sqrt{z}$, and $R = I_1(\sqrt{z})$, and carrying out the appropriate operations, one finds that the RHS yields $\Sigma\,\mathcal{R} = 2\exp(-\tau\mu_n^2)J_0(\mu_n\eta)/J_0(\mu_n)$, where μ_n is the nth root of the characteristic equation, $J_1(\mu_n) = 0$. Hence, the inverse formula of Eq. (A3) occurs in the form of a Volterra integral equation of the second kind given by Eq. (2).

For the time-dependent side condition, similar steps have to be taken to reach the equivalent of Eq. (A3), which in this situation happens to be given by

$$\theta(\tau,\eta) = -\frac{Po}{Pd}(1 - e^{-Pd\tau}) - Bi_0 l^{-1}\left\{\left[\bar{\theta}(1,s) - \bar{\theta}(1,s+A) - \frac{A}{s(s+A)}\right]\frac{I_0(\eta\sqrt{s})}{\sqrt{s}I_1(\sqrt{s})}\right\} \tag{A11}$$

Applying the convolution theorem to this equation, the desired integral equation, Eq. (3), is obtained.

References

[1]Tokuda, N., "A New Application of Lagrange-Brumann Expansions II. Application to Unsteady Heat Conduction Problems with Radiation," *Journal of Applied Mathematics and Physics*, Vol. 34, Nov. 1983, pp. 787–806.

[2]Becker, N. M., Bivins, R. L., Hsu, Y. C., Murphy, H. D., White, A. B., and Wing, G. M., "Heat Diffusion with Time-Dependent Convective Boundary Conditions," *International Journal for Numerical Methods in Engineering*, Vol. 19, Aug. 1983, pp. 1871–1880.

[3]"PHOENICS," Concentration Heat & Momentum Limited, Wimbledon Village, London, 1995.

[4]Apelian, D., Gillen, G., and Leatham, A. G., *In Processing of Structural Metals by Rapid Solidification*, edited by F. H. Froes and S. J. Savage, American Society for Microbiology, Metals Park, OH, 1987.

[5]Siegel, R., "Transient Radiative Cooling of a Droplet-Filled Layer," *Journal of Heat Transfer*, Vol. 109, No. 1, 1987, pp. 159–164.

[6]Bayazitoglu, Y., Suryanarayana, P. V. R., and Sathuvalli, U. B., *Journal of Thermophysics and Heat Transfer*, Vol. 4, No. 4, 1990, pp. 462–468.

[7]Chambre, P. E., "Nonlinear Heat Transfer Problem," *Journal of Applied Physics*, Vol. 30, No. 11, 1959, pp. 1683–1688.

[8]Abarbanel, S. S., "The Radiating Sphere," *On Some Problems in Radiative Heat Transfer*, Massachusetts Inst. of Technology, Fluid Dynamics Research Group, OSR. TN, 1959, Cambridge, MA, pp. 42–50.

[9]Crosbie, A. L., and Viskanta, R., "A Simplified Method for Solving Transient Heat-Conduction Problems with Nonlinear Boundary Conditions," *Journal of Heat Transfer*, Vol. 90, Aug. 1968, pp. 358, 359.

[10]Van der Houwen, P. J., and Te Riele, H. J. J., "Linear Multistep Methods for Volterra Integral Equations of the Second Kind," *Treatment of Integral Equations by Numerical Methods*, 1st ed., Academic, London, 1982, pp. 79–93.

[11]Lubich, C., "On the Stability of Linear Multistep Methods for Volterra Integral Equations of the Second Kind," *Treatment of Integral Equations by Numerical Methods*, 1st ed., Academic, London, 1982, pp. 233–238.

[12]Amini, S., "On the Stability of Numerical Methods for Volterra Integral Equations of the Second Kind," *Treatment of Integral Equations by Numerical Methods*, 1st ed., Academic, London, 1982, pp. 43–46.

[13]Lubich, C., "On the Stability of Linear Multistep Methods for Volterra Convolution Equations," *Institute of Mathematics and its Applications*, Vol. 3, No. 3, 1983, pp. 439–465.

[14]Blom, J. G., and Brunner, H., "Algorithm 689: Discretized Collocation and Iterated Collocation for Nonlinear Volterra Integral Equations of the Second Kind," *Association for Computing Machinery*, Vol. 17, No. 2, 1991, pp. 167–177.

[15]Crosbie, A. L., and Viskanta, R., "Transient Heating or Cooling of a Plate by Combined Convection and Radiation," *International Journal of Heat and Mass Transfer*, Vol. 11, 1968, pp. 305–317.

[16]Canuto, C., Hussaini, M. Y., Quarteroni, A., and Zang, T. A., "Spectral Approximation," *Spectral Methods in Fluid Dynamics*, 2nd ed., Springer–Verlag, Berlin, 1988, pp. 31–75.

[17]Luikov, A. V., "Temperature Field with Continuous Heat Source," *Heat Conduction Theory*, 2nd ed., Vyssh. Shkola, Moscow, Russia, 1967, pp. 351–376.

[18]Baker, C. T. H., "Volterra Equations," *The Numerical Treatment of Integral Equations*, 2nd ed., Thomson Litho Ltd., Scotland, UK, 1977, pp. 754–827.

[19]Van der Houwen, P. J., and Te Riele, H. J. J., "Linear Multistep Methods for Volterra Integral and Integro-Differential Equations," *Mathematics of Computation*, Vol. 45, March 1985, pp. 439–461.

[20]Abramowitz, M., and Stegun, I. A., *Handbook of Mathematical Functions*, 10th ed., Dover, New York, 1972, pp. 358–494.

[21]Linz, P., *Analytical and Numerical Methods for Volterra Equations*, Taylor and Francis, Washington, DC, 1985.

[22]Hoffmann, K. A., "Parabolic Partial Differential Equations," *Computational Fluid Dynamics for Engineers*, 1st ed., Engineering Education System, Austin, TX, 1989, pp. 50–96.